

## Porphyrinoids

International Edition: DOI: 10.1002/anie.201607237  
German Edition: DOI: 10.1002/ange.201607237

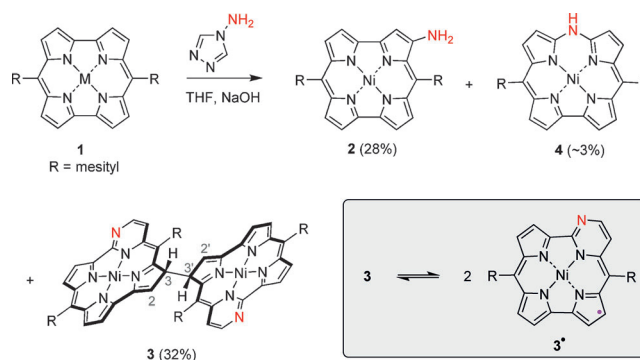
## Reversible Carbon–Carbon Bond Breaking and Spin Equilibria in Bis(pyrimidinenorcorrole)

Bin Liu, Takuya Yoshida, Xiaofang Li,\* Marcin Stepień, Hiroshi Shinokubo, and Piotr J. Chmielewski\*

**Abstract:** Reversible homolytic dissociation of the bis(pyrimidinenorcorrole)  $\sigma$ -dimer was elucidated by means of variable temperature ESR and  $^1\text{H}$  NMR spectroscopy, mass spectrometry, and optical spectroscopy. Dehydrogenation of the  $\sigma$ -dimer yielded another dimer displaying a singlet–triplet equilibrium in solution, strong NIR absorption (1570 nm), and a narrow electrochemical HOMO–LUMO gap (0.74 V).

Reversible dissociation of carbon–carbon bonds has attracted considerable attention because of the theoretical and experimental significance of this phenomenon in various areas of chemistry.<sup>[1–3]</sup> In some instances, the bonded and dissociated state are so close in energy that dynamic bond breaking occurs rapidly under ambient conditions;<sup>[1]</sup> otherwise, an external stimulus (thermal or photochemical) is required to drive the process.<sup>[3]</sup> Intramolecular dissociation can be particularly facile, leading to various rearrangement reactions.<sup>[1e,f,j,2,3a,c,e,g–k]</sup> However, the most intriguing processes are those occurring in an intermolecular fashion as they provide access to unique dynamic structures, such as self-healing polymers.<sup>[1b]</sup> Here we report a bis(porphyrinoid), linked through a  $\text{C}(\text{sp}^3)\text{--}\text{C}(\text{sp}^3)$  bond, which exists in solution in an equilibrium with the corresponding monomeric radical. This hemilabile dimer can be dehydrogenated to a  $\text{C}(\text{sp}^2)=\text{C}(\text{sp}^2)$ -linked bis(porphyrinoid) species, which demonstrates a singlet–triplet spin equilibrium associated with conformational decoupling of the two porphyrinoid  $\pi$  systems.

Nickel(II) norcorrole **1** is a recently discovered 16- $\pi$ -electron tetrapyrrolic porphyrinoid, which displays an antiaromatic character and a reactivity quite distinct from that of aromatic oligopyrroles.<sup>[4–6]</sup> In an attempt to introduce an  $\text{NH}_2$  group into **1**, we employed 4*H*-1,2,4-triazol-4-amine<sup>[7]</sup> in the presence of solid sodium hydroxide in THF (Scheme 1). The



**Scheme 1.** Amination of norcorrolatonickel(II) and dissociation of **3** into monomer radical **3**.

amination proceeded with the regioselectivity observed previously for cyanation<sup>[5c]</sup> and nitration<sup>[6b]</sup> providing 3-aminonorcorrolatonickel(II) **2** in 28% yield. To our surprise, two additional products were formed due to ring expansion, which were the dimeric species **3** (32%) and the previously reported<sup>[8]</sup> 10-azacorrolatonickel(II)**4** (ca. 3%). All compounds were unambiguously identified and characterized using NMR and HRMS spectra, and in the case of **2**, also by single-crystal X-ray diffraction analysis (Figure S33, CCDC 1479588 contains the supplementary crystallographic data for this paper. These data can be obtained free of charge from The Cambridge Crystallographic Data Centre).

In contrast to the parent antiaromatic norcorrole complex **1** and its amination product **2**, the dimeric species **3** is non-aromatic because the formation of the  $\beta\text{--}\beta$  linkage disrupts the macrocyclic conjugation in both subunits. The most distinctive feature of the  $^1\text{H}$  NMR spectrum of **3** (Figure S6a) is an AA'XX' system of H2(2') and H3(3') which gives rise to characteristic multiplets at  $\delta$  5.87 and 3.83 ppm (600 MHz, 300 K,  $\text{CDCl}_3$ ), in line with the presence of isochronous, yet magnetically non-equivalent protons, and thus, with the dimeric structure of **3**. Further structural details, such as the presence of  $\text{sp}^3$  carbon atoms at the bridging bond, the presence of six-membered ring of pyrimidine, non-planarity of the system, and the location of the bridge relative to the pyrimidine ring, were established by means of 1D and 2D homo- and heteronuclear NMR techniques. The NMR spectra of **3** correspond to an effective  $C_2$  symmetry of the dimer (with homochiral C3 and C3' stereocenters) rather than  $C_i$  (with heterochiral stereocenters), according to energy-minimized DFT models of these two diastereomers and variable-temperature experiments (173–300 K,  $\text{CD}_2\text{Cl}_2$ ). Despite the presence of two homochiral centers in **3**, the

[\*] B. Liu, Prof. X. Li  
Key Laboratory of Theoretical Organic Chemistry and  
Functional Molecules, Ministry of Education  
School of Chemistry and Chemical Engineering  
Hunan University of Science and Technology  
Xiangtan, Hunan 411201 (China)  
E-mail: lixiaofang@iccas.ac.cn

T. Yoshida, Prof. H. Shinokubo  
Department of Applied Chemistry, Graduate School of Engineering  
Nagoya University, Nagoya 464-8603 (Japan)

Prof. M. Stepień, Prof. P. J. Chmielewski  
Department of Chemistry, University of Wrocław  
F. Joliot-Curie 14, 50383 Wrocław (Poland)  
E-mail: piotr.chmielewski@chem.uni.wroc.pl

Supporting information for this article can be found under:  
<http://dx.doi.org/10.1002/anie.201607237>.

enantiomers could not be separated by chiral HPLC which suggested that the stereocenters in **3** might be configurationally unstable. The positive-mode ESI and MALDI mass spectra of **3** revealed the molecular ion at  $m/z = 1181.37$  ( $[M+H]^+$ ) and an additional, singly charged peak at  $m/z = 590.19$ , corresponding to  $[M/2]^+$ . A peak with an essentially the same  $m/z$  ratio was also found in the negative-mode spectra, providing further support for the dissociation of the C3–C3' linkage in **3** occurring in the ion source.

The weakness of the C3–C3' bond in the dimer was further demonstrated to result in reversible homolytic dissociation of **3** in solution. The optical spectrum of **3** was significantly altered upon heating, and the toluene solution changed its color from grass-green at room temperature to olive-brown at 353 K (Figure 1A). Variable-temperature ESR spectra of **3**

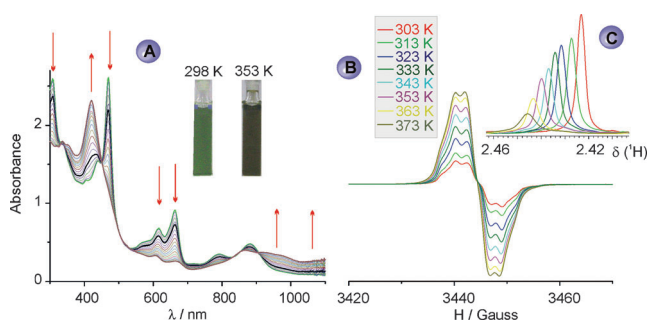


**Figure 1.** A) Temperature dependence of the UV/Vis-NIR spectra of **3** ( $2.85 \times 10^{-4}$  M in toluene) in the range from 274 K (green trace) to 368 K (brown trace). The bold black line is the spectrum recorded at 298 K. B) ESR spectra of the toluene solution of **3** recorded at specified temperatures. C) The inset shows  $^1\text{H}$  NMR signals of protons 5-*p*-Mes of **3** at specified temperatures ( $[\text{D}_8]\text{toluene}$ , normalized intensity spectra).

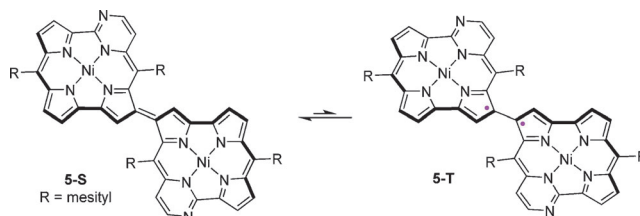
recorded in a toluene solution, revealed the presence of a radical species at room temperature, with a gradual, up to six-fold increase of the signal intensity observed on going to 100 °C (Figure 1B). The intensity of  $^1\text{H}$  NMR signals appreciably decreased with respect to an internal standard as the temperature increased, though chemical shifts of the signals varied only slightly over the whole temperature range ( $[\text{D}_8]\text{toluene}$ , 253–373 K), likely due to changes in solvation (Figure 1C). These observations are indicative of a chemical exchange, which is slow on the NMR time scale, between the diamagnetic **3** and the radical dissociation product **3** $\cdot$ , the latter yielding NMR spectral lines that are too broad to be detected. The radical content, estimated on the basis of  $^1\text{H}$  NMR signal integration, increased from about 12% at 300 K to almost 90% at 373 K. All spectral changes induced by increasing the temperature were fully reversed upon cooling and the cycle could be reproduced many times under anaerobic conditions.

The response of the system to the temperature changes was not instantaneous. Kinetics of the dissociation and recombination processes were studied spectrophotometrically in the temperature range of 30 to 45 °C, providing rate constants  $k_{\text{diss}} = 1.36 \times 10^{-2}$ – $3.00 \times 10^{-2}$  s $^{-1}$  and  $k_{\text{rec}} = 1.62 \times 10^{-2}$ – $2.60 \times 10^{-2}$  s $^{-1}$  and activation energies  $E_a = 10 \pm 1$  kcal

mol $^{-1}$  for dissociation and  $E_a = 5 \pm 1$  kcal mol $^{-1}$  for recombination. The reactions in both directions were first-order, indicating that for the recombination, the rate-determining step might be associated with a structural change (likely, a  $\pi$ -dimer-to- $\sigma$ -dimer rearrangement) that follows the actual dimerization. Thermodynamic parameters for the dissociation were determined by variable-temperature spectrophotometry and values of  $\Delta H^0 = 20.2 \pm 1.5$  kcal mol $^{-1}$ ,  $\Delta S^0 = 46 \pm 3$  cal mol $^{-1}$  K $^{-1}$  and  $\Delta G^0_{298} = 6.5 \pm 2.4$  kcal mol $^{-1}$  were determined from the van't Hoff equation.

The free-energy changes due to dissociation derived from DFT calculations using the  $\omega\text{B97XD}$  functional were consistent with the experimentally observed reversibility of the process (counterpoise-corrected free energy  $\Delta G^0_{298} = 3.92$  kcal mol $^{-1}$ ). The DFT-optimized structure of the radical **3** $\cdot$ , showed complete planarization of all  $\beta$ -pyrrole carbons, reflecting the restored peripheral conjugation in the macrocycle. The calculated spin distribution in **3** $\cdot$  had a negligible intensity at the Ni center, and the unpaired electron was mostly placed on the *meso*-carbons C5, C15 as well as on C1-C4, C11, and C19 (Figure S21), confirming the  $\pi$ -radical character of **3** $\cdot$ . Appreciable Fermi contacts were calculated by DFT for proton atoms H2, H3, H8, and H13 ( $a_H = 2.82$ ,  $-10.60$ ,  $-3.16$ , and  $-6.02$  MHz, respectively) and nitrogen atoms N21 as well as N23 ( $a_N = 9.00$ , 4.38 MHz, respectively). The calculated spin distribution slightly differs from that observed experimentally, since the ESR spectrum was best reproduced by simulation assuming interaction of the unpaired electron with two equivalent nitrogen atoms ( $a_N = 6.37$  MHz) and four hydrogen atoms ( $a_H = 6.23$ , 3.00, 2.44 (2H) MHz, Figure S21).

In polar solvents, the green dimer **3** underwent a further irreversible transformation to a brown product **5**, containing the dehydrogenated C3–C3' linkage (Scheme 2). The reaction



**Scheme 2.** Singlet–triplet equilibrium in **5**.

was particularly effective when carried out in DMF giving quantitative conversion over 30 minutes at 80 °C; in acetonitrile, the dehydrogenation took place at room temperature, yielding crystalline product in moderate yield after four days. The process is likely due to the presence of atmospheric oxygen acting as a dehydrogenating agent, although the reaction can be conducted also in less polar solvents under catalytic and rigorously anaerobic conditions (60 °C, toluene, glove box, Pd/C, 3 h, 50% yield). The loss of two hydrogen atoms in **5** was confirmed by HRMS and its structure was fully elucidated by a single-crystal X-ray diffraction analysis (Figure 2A, CCDC 1479589 contains the supplementary crystallographic data for this paper. These data can be obtained free

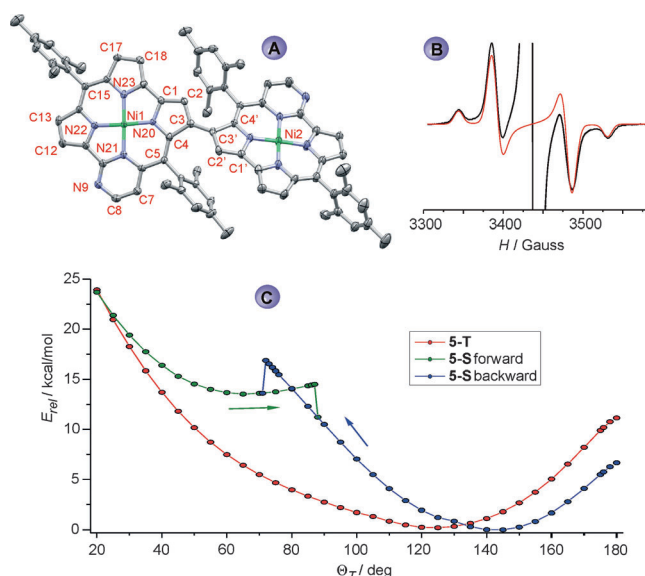


**Figure 2.** A) Molecular structure of **5** depicted with 50% thermal ellipsoids. All hydrogen atoms are omitted. B) ESR spectrum of solid **5** at 77 K. Red trace: simulation of the  $S=1$  system. C) Relaxed DFT potential energy surface scans for **5-S** (blue and green circles) and **5-T** (red circles) on  $\text{C2-C3-C3'-C2'}$  torsion angle  $\theta_T$ .

of charge from The Cambridge Crystallographic Data Centre.). In solid state, **5** consists of two flat macrocyclic subunits (with mean out-of-plane displacements of 0.052 and 0.069 Å) forming a dihedral angle  $\theta_D$  of  $44.0^\circ$  and a  $\text{C2-C3-C3'-C2'}$  torsion  $\theta_T$  of  $143.9(4)^\circ$ . The unique  $\text{C3-C3'}$  bond has a length of 1.437(5) Å, which is appreciably shorter than bond lengths reported for  $\beta,\beta'$ -linked bis(porphyrins) (1.46–1.47 Å),<sup>[9]</sup>  $N$ -confused porphyrin dimers (1.463–1.490 Å),<sup>[10]</sup> bis(corrole) free base (1.490(8) Å),<sup>[11a]</sup> porphyrin-chlorin heterodimer (1.522(5)),<sup>[11b]</sup> bis(chlorin) (1.61 Å),<sup>[12]</sup> or  $\text{C}_{meso}$ – $\text{C}_{meso}$  bond in bis(porphyrin) complexes (1.47–1.51 Å)<sup>[13]</sup> all consisting of aromatic subunits linked by a single bond and containing an even number of delocalized  $\pi$ -electrons in each macrocyclic ring. Conversely, in **5**, each macrocyclic  $\pi$ -system contains 19  $\pi$ -electrons, so that two electrons need to be paired across the  $\text{C3-C3'}$  bond to yield a closed-shell system. The non-coplanarity of subunits in **5** was nevertheless thought to destabilize the interannular  $\pi$ -conjugation, with the expectation that the electrons might become unpaired and yield two weakly interacting 19-electron systems. Interestingly, **5** was found to be weakly paramagnetic in solid state, with an effective magnetic moment  $\mu_{eff}$  of  $0.58 \mu_B$  at 1.8 K, which increases up to  $0.70 \mu_B$  at 50 K without any further systematic change up to 300 K. Thus, a small part of compound **5** is in a paramagnetic state but exchange interaction between the unpaired electrons appears to be weak. From a triplet-state spin-only magnetic moment ( $2.83 \mu_B$ ), the estimated content of the paramagnetic species at room temperature is about 6%. The present system differs from a diradical generated for a doubly linked bis(corrole), wherein a strong exchange interaction completely quenched the spin below 150 K in the solid state.<sup>[14]</sup> The ESR spectrum of solid **5** at 77 K displayed a signal typical of triplet-state biradicals<sup>[15]</sup> ( $g_{\parallel} = 2.0018$ ,  $g_{\perp} =$

$2.0026$ ,  $D = 0.0095 \text{ cm}^{-1}$ ), apart from a featureless radical signal which may arise upon sample preparation through spontaneous oxidation of **5** (Figure 2B). No  $\Delta m_s = 2$  line was observed. The rather small zero-field splitting parameter  $D$  is consistent with the nonplanar structure of the dimer<sup>[14]</sup> and indicates a weak dipolar interaction between the radical centers.<sup>[15]</sup> That in turn, suggests separate delocalization of the spin over each of the subunits.

<sup>1</sup>H NMR spectroscopy in solution indicates a fast chemical exchange between the diamagnetic and paramagnetic species, resulting in temperature-dependent variations of chemical shifts, line widths, and longitudinal relaxation times  $T_1$ , observed for most resonances (Figures S24–S27). At low temperatures (183 K,  $\text{CD}_2\text{Cl}_2$ ), all signals are reasonably sharp and can be assigned by 2D techniques, and their spin-lattice relaxation times ( $T_1 > 1 \text{ s}$ ) are typical for diamagnetic species. At room temperature, however, some signals (e.g. H8 and H13) are extremely broadened and unobservable, while others, such as H17 and H18, remain sharp enough to reveal spin–spin splittings. All  $T_1$  relaxation times at 300 K are much shorter than those observed at 183 K (0.04–0.5 s), in line with the higher population of the paramagnetic form and/or faster chemical exchange between the forms. Significantly, below 203 K, there are six distinct methyl signals of the *meso*-mesityl substituents, proving that the rotation at the  $\text{C3-C3'}$  bond is frozen. The rotation becomes rapid at higher temperatures, resulting in pairwise averaging of the *o*-Mes signals. The frequency of rotation around the  $\text{C3-C3'}$  bond can be estimated as about 340–370 Hz at the coalescence temperatures of individual signals reflecting flexibility of the molecular skeleton. That kind of structural flexibility prevents the chromatographic separation of atropisomers observed in the solid state by X-ray diffraction.<sup>[9b,10a,e]</sup> Unlike **3**, dimer **5** revealed only weak temperature dependence of its optical spectra (25–100°C, toluene) with only a slight increase of absorption at 416 nm and a similar decrease at 950 nm (Figure S28). These observations reflect a small contribution of **5-T** over the whole temperature range.

DFT calculations were carried out for **5** in open- and closed-shell singlet (**5-S**) and triplet (**5-T**) states. Since the open-shell singlet (modeled using the broken-symmetry approach) gave no stable SCF solutions, we confined our analysis to the restricted and unrestricted Hartree–Fock approximation for **5-S** and **5-T**, respectively (Scheme 2). The optimized geometry of **5-S** (more stable by  $0.39 \text{ kcal mol}^{-1}$  than **5-T**) reproduces closely the features of the X-ray structure ( $r_{\text{C3-C3'}} = 1.417 \text{ Å}$ ;  $\text{C2-C3-C3'-C2'}$  torsion  $\theta_T = 142.8^\circ$ ; dihedral angle  $\theta_D = 42.3^\circ$ ). The optimized structure of **5-T** is characterized by a significantly longer  $\text{C3-C3'}$  bond (1.468 Å), lower  $\theta_T$  torsion ( $120.5^\circ$ ), and higher dihedral angle between the mean planes ( $\theta_D = 61.5^\circ$ ). Relaxed potential-energy scans performed along the  $\theta_T$  coordinate for **5-S** and **5-T** ( $\theta_T = 20$  to  $180^\circ$ ) indicated that the triplet ground state is preferred for the more perpendicular orientations of the macrocyclic subunits ( $25 < \theta_T < 135^\circ$  or  $47 < \theta_D < 90^\circ$ ). The  $E(\mathbf{5-S}) - E(\mathbf{5-T})$  energy gap reaches  $8\text{--}10 \text{ kcal mol}^{-1}$  at the near-perpendicular orientation of the subunits ( $\theta_T = 70\text{--}90^\circ$ , Figure 2C), with the  $\text{C3-C3'}$  bond length in **5-S** sharply increasing up to 1.48 Å, a value typical for a single  $\text{C}(\text{sp}^2)\text{--}$

C(sp<sup>2</sup>) bond (Figure S35). Thus, the observed energy increase might in part be attributed to the strain introduced to the C3–C3' double bond in **5-S**. The calculation of spin distribution in the energy-minimized structure of **5-T** indicates the highest spin density at *meso*-carbon atoms of both subunits (C5, C15, C5', and C15'), bridging C3, C3', and internal nitrogen atoms N21, N21' (pyrimidine) and N23, N23'. Altogether, the spin distribution over each subunit closely resembles that calculated for **3'** and roughly correlates with line widths,  $T_1$  values, and the temperature dependence of <sup>1</sup>H NMR chemical shifts for the corresponding protons of **5** (Figures S24–S27).

Electrochemical measurements for **5** indicate an interaction between the subunits, which appears to be stronger than in singly-bonded bis(porphyrinoids).<sup>[6a,9b,10a,e]</sup> Two reversible oxidation couples ( $E_{1/2} = -0.10$  and  $0.11$  V) and two reduction couples ( $E_{1/2} = -0.84$  and  $-1.05$  V), accompanied by the less accessible redox events at  $1.02$  V and  $-2.22$  V were observed for **5** in CH<sub>2</sub>Cl<sub>2</sub> (potentials vs. the internal ferrocene standard). The narrow electrochemical HOMO–LUMO gap ( $\Delta E = 0.74$  V) is in line with that predicted by DFT calculations ( $1.08$  eV) and with the NIR absorption of **5** with an onset of the lowest-energy band reaching  $1700$  nm (ca.  $0.73$  eV, Figure S30).

In conclusion, we have shown here an unprecedented ring expansion of norcorrole which provides a straightforward access to two spin-switchable bis(porphyrinoid) systems. These two dimers, each consisting of two pyrimidine-containing norcorrole rings, undergo reversible homolytic cleavage of either a  $\sigma$ -bond or a  $\pi$ -bond, depending on the oxidation level, thus leading to two distinct types of magnetic bistability. It is likely that such equilibria are more common but seldom identified and they may be responsible for the reactivity of diverse  $\pi$ -aromatics. Considering the renewed interest in functional organic radicals, usable as switches or dynamic building blocks,<sup>[1a–d,2,3b,15d,16]</sup> the reactivity of **3'** and the coordination chemistry of the dimer **5**, in conjunction with its ability to adopt various oxidation and spin states, are particularly attractive and will be further explored in our laboratories.

## Acknowledgements

This work was supported by the National Natural Science Foundation of China (Nos. 21371054 and 21671063), the Scientific Research Fund of Hunan Provincial Education Department (grant number 13A026), and by the Polish National Science Center (grant number 2013/09/B/ST5/00326). Quantum chemical calculations were performed in the Wrocław and Poznań Centers for Networking and Supercomputing.

**Keywords:** biradicals · free-radical dimerization · norcorrole · porphyrinoids · spin equilibria

- [1] a) M. W. Urban, *Nat. Chem.* **2012**, *4*, 80–82; b) K. Imato, M. Nishihara, T. Kanehara, Y. Amamoto, A. Takahara, H. Otsuka, *Angew. Chem. Int. Ed.* **2012**, *51*, 1138–1142; *Angew. Chem.* **2012**, *124*, 1164–1168; c) C. J. Allan, B. F. T. Cooper, H. J. Cowley, J. M. Rawson, C. L. B. Macdonald, *Chem. Eur. J.* **2013**, *19*, 14470–14483; d) D. Beaudoin, O. Levasseur-Grenon, T. Maris, J. D. Wuest, *Angew. Chem. Int. Ed.* **2016**, *55*, 894–898; *Angew. Chem.* **2016**, *128*, 906–910; e) T. Kawamoto, N. Suzuki, T. Ono, D. Gong, T. Konno, *Chem. Commun.* **2013**, *49*, 668–670; f) K. J. Jonasson, A. V. Polukeev, R. Marcos, M. S. G. Ahlquist, O. F. Wendt, *Angew. Chem. Int. Ed.* **2015**, *54*, 9372–9375; *Angew. Chem.* **2015**, *127*, 9504–9507; g) R. A. Lewis, K. C. MacLeod, B. Q. Mercado, P. L. Holland, *Chem. Commun.* **2014**, *50*, 11114–11117; h) G. Nocton, L. Ricard, *Chem. Commun.* **2015**, *51*, 3578–3581; i) G. Nocton, W. W. Lukens, C. H. Booth, S. S. Rozenel, S. A. Medling, L. Maron, R. A. Andersen, *J. Am. Chem. Soc.* **2014**, *136*, 8626–8641; j) M. J. Monreal, P. L. Diaconescu, *J. Am. Chem. Soc.* **2010**, *132*, 7676–7683; k) R. Dugan, E. Bill, K. C. McLeod, G. J. Christian, R. E. Cowley, W. W. Brennessel, S. Ye, F. Neese, P. L. Holland, *J. Am. Chem. Soc.* **2012**, *134*, 20352–20364; l) J. M. Wittman, R. Hayoun, W. Kaminsky, M. K. Coggins, J. M. Mayer, *J. Am. Chem. Soc.* **2013**, *135*, 12956–12959.
- [2] K. Uchida, M. Ito, M. Abe, T. Kubo, *J. Am. Chem. Soc.* **2016**, *138*, 2399–2410.
- [3] a) C. A. Huff, J. W. Kampf, M. S. Sanford, *Chem. Commun.* **2013**, *49*, 7147–7149; b) C. C. Hojilla Atienza, C. Milsman, S. P. Semproni, Z. R. Turner, P. J. Chirik, *Inorg. Chem.* **2013**, *52*, 5403–5417; c) M. Montag, J. Zhang, D. Milstein, *J. Am. Chem. Soc.* **2012**, *134*, 10325–10328; d) M. H. Shaw, N. G. McCreanor, W. G. Whittingham, J. F. Bower, *J. Am. Chem. Soc.* **2015**, *137*, 463–468; e) M. Vogt, A. Nerush, M. A. Iron, G. Leitus, Y. Diskin-Posner, L. J. Shimon, Y. Ben-David, D. Milstein, *J. Am. Chem. Soc.* **2013**, *135*, 17004–17018; f) S. Kulchat, K. Meguelati, J.-M. Lehn, *Helv. Chim. Acta* **2014**, *97*, 1219–1236; g) T. Suzuki, T. Takeda, E. Ohta, K. Wada, R. Katoono, H. Kawai, K. Fujiwara, *Chem. Rec.* **2015**, *15*, 280–294; h) Y.-L. Rao, H. Amarne, S.-B. Zhao, T. M. McCormick, S. Martić, Y. Sun, R.-Y. Wang, S. Wang, *J. Am. Chem. Soc.* **2008**, *130*, 12898–12900; i) M. Vogt, M. Gargir, M. A. Iron, Y. Diskin-Posner, Y. Ben-David, D. Milstein, *Chem. Eur. J.* **2012**, *18*, 9194–9197; j) J. Bachmann, D. G. Nocera, *J. Am. Chem. Soc.* **2005**, *127*, 4730–4743; k) J. Bachmann, D. G. Nocera, *J. Am. Chem. Soc.* **2004**, *126*, 2829–2837.
- [4] M. Bröring, S. Köhler, C. Kleeberg, *Angew. Chem. Int. Ed.* **2008**, *47*, 5658–5660; *Angew. Chem.* **2008**, *120*, 5740–5743.
- [5] a) T. Fukuoka, K. Uchida, Y. M. Sung, J.-Y. Shin, S. Ishida, J. M. Lim, S. Hiroto, K. Furukawa, D. Kim, T. Iwamoto, H. Shinokubo, *Angew. Chem. Int. Ed.* **2014**, *53*, 1506–1509; *Angew. Chem.* **2014**, *126*, 1532–1535; b) T. Ito, Y. Hayashi, S. Shimizu, J.-Y. Shin, N. Kobayashi, H. Shinokubo, *Angew. Chem. Int. Ed.* **2012**, *51*, 8542–8545; *Angew. Chem.* **2012**, *124*, 8670–8673; c) R. Nozawa, K. Yamamoto, J.-Y. Shin, S. Hiroto, H. Shinokubo, *Angew. Chem. Int. Ed.* **2015**, *54*, 8454–8457; *Angew. Chem.* **2015**, *127*, 8574–8577; d) J.-Y. Shin, T. Yamada, H. Yoshikawa, K. Awaga, H. Shinokubo, *Angew. Chem. Int. Ed.* **2014**, *53*, 3096–3101; *Angew. Chem.* **2014**, *126*, 3160–3165.
- [6] a) B. Liu, X. Li, M. Stepień, P. J. Chmielewski, *Chem. Eur. J.* **2015**, *21*, 7790–7797; b) Z. Deng, X. Li, M. Stepień, P. J. Chmielewski, *Chem. Eur. J.* **2016**, *22*, 4231–4246.
- [7] a) A. R. Katritzky, K. S. Laurenzo, *J. Org. Chem.* **1988**, *53*, 3978–3982; b) S. Richeter, C. Jeandon, J.-P. Gisselbrecht, R. Ruppert, H. J. Callot, *J. Am. Chem. Soc.* **2002**, *124*, 6168–6179; c) S. Richeter, C. Jeandon, J.-P. Gisselbrecht, R. Graff, R. Ruppert, H. J. Callot, *Inorg. Chem.* **2004**, *43*, 251–263; d) S. Richeter, C. Jeandon, J.-P. Gisselbrecht, H. J. Callot, *Inorg. Chem.* **2007**, *46*,

- 10241–10251; e) J.-F. Lefebvre, D. Leclercq, J.-P. Gisselbrecht, S. Richeter, *Eur. J. Org. Chem.* **2010**, 1920; f) S. Richeter, A. Hadj-Aissa, C. Taffin, A. van der Lee, D. Leclercq, *Chem. Commun.* **2007**, 2148–2150; g) R. Tiwari, M. Nath, *New J. Chem.* **2015**, 39, 5500–5506; h) M. Stefanelli, F. Mandoj, M. Mastroianni, S. Nardis, P. Mohite, F. R. Fronczek, K. M. Smith, K. M. Kadish, X. Xiao, Z. Ou, P. Chen, R. Paolesse, *Inorg. Chem.* **2011**, 50, 8281–8292.
- [8] M. Horie, Y. Hayashi, S. Yamaguchi, H. Shinokubo, *Chem. Eur. J.* **2012**, 18, 5919–5923.
- [9] a) Y. Deng, C. K. Chang, D. G. Nocera, *Angew. Chem. Int. Ed.* **2000**, 39, 1066; *Angew. Chem.* **2000**, 112, 1108; b) G. Bringmann, D. C. G. Goetz, T. A. M. Gulder, T. H. Gehrke, T. Bruhn, T. Kupfer, K. Radacki, H. Braunschweig, A. Heckmann, C. Lambert, *J. Am. Chem. Soc.* **2008**, 130, 17812–17825.
- [10] a) P. J. Chmielewski, *Angew. Chem. Int. Ed.* **2004**, 43, 5655–5658; *Angew. Chem.* **2004**, 116, 5773–5776; b) P. J. Chmielewski, M. Siczek, L. Szterenber, *Inorg. Chem.* **2011**, 50, 6719–6736; c) P. J. Chmielewski, *Angew. Chem. Int. Ed.* **2005**, 44, 6417–6420; *Angew. Chem.* **2005**, 117, 6575–6578; d) M. Siczek, P. J. Chmielewski, *Angew. Chem. Int. Ed.* **2007**, 46, 7432–7436; *Angew. Chem.* **2007**, 119, 7576–7580; e) P. J. Chmielewski, J. Maciolek, *Chem. Commun.* **2012**, 48, 428–430.
- [11] a) S. Hirabayashi, M. Omote, N. Aratani, A. Osuka, *Bull. Chem. Soc. Jpn.* **2012**, 85, 558–562; b) X. Kai, J. Jiang, C. Hu, *Chem. Commun.* **2012**, 48, 4302–4304.
- [12] B. Krattinger, D. J. Nurco, K. M. Smith, *Chem. Commun.* **1998**, 757–758.
- [13] N. Yoshida, T. Ishizuka, A. Osuka, D. H. Jeong, H. S. Cho, D. Kim, Y. Matsuzaki, A. Nogami, K. Tanaka, *Chem. Eur. J.* **2003**, 9, 58–75.
- [14] S. Hiroto, K. Furukawa, H. Shinokubo, A. Osuka, *J. Am. Chem. Soc.* **2006**, 128, 12380–12381.
- [15] a) M. Abe, *Chem. Rev.* **2013**, 113, 7011–7088; b) D. A. Shultz, C. P. Mussari, K. K. Ramanathan, J. W. Kampf, *Inorg. Chem.* **2006**, 45, 5752–5759; c) Z. Zeng, X. Shi, C. Chi, J. T. L. Navarrete, J. Casado, J. Wu, *Chem. Soc. Rev.* **2015**, 44, 6578–6596; d) D. Shimizu, J. Oh, K. Furukawa, D. Kim, A. Osuka, *J. Am. Chem. Soc.* **2015**, 137, 15584–15594.
- [16] a) K. Kato, W. Cha, J. Oh, K. Furukawa, H. Yorimitsu, D. Kim, A. Osuka, *Angew. Chem. Int. Ed.* **2016**, 55, 8711–8714; *Angew. Chem.* **2016**, 128, 8853–8856; b) M. Ishida, J.-Y. Shin, J.-M. Lim, B. S. Lee, M.-C. Yoon, T. Koide, J. L. Sessler, A. Osuka, D. Kim, *J. Am. Chem. Soc.* **2011**, 133, 15544; c) T. Koide, G. Kashiwazaki, M. Suzuki, K. Furukawa, M.-C. Yoon, S. Cho, D. Kim, A. Osuka, *Angew. Chem. Int. Ed.* **2008**, 47, 9661–9665; *Angew. Chem.* **2008**, 120, 9807–9811; d) P. Schweyen, K. Brandhorst, R. Wicht, B. Wolfram, M. Bröring, *Angew. Chem. Int. Ed.* **2015**, 54, 8213–8216; *Angew. Chem.* **2015**, 127, 8331–8334; e) T. Y. Gopalakrishna, J. S. Reddy, V. G. Anand, *Angew. Chem. Int. Ed.* **2014**, 53, 10984–10987; *Angew. Chem.* **2014**, 126, 11164–11167.

Received: July 26, 2016

Published online: ■■■■■, ■■■■■

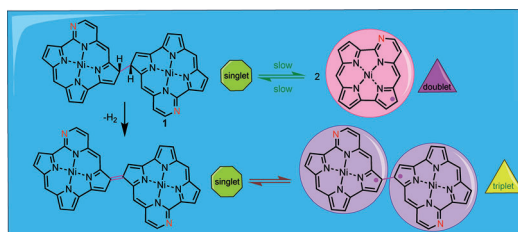
## Communications



## Porphyrinoids

B. Liu, T. Yoshida, X. Li,\* M. Stępień,  
H. Shinokubo,  
P. J. Chmielewski\* ———— ■■■■-■■■■

Reversible Carbon–Carbon Bond  
Breaking and Spin Equilibria in  
Bis(pyrimidinenorcorrole)



**Porphyrinoid metal complexes:** Amination of the nickel(II) complex of norcorrole under mild conditions resulted in C(sp<sup>3</sup>)-C(sp<sup>3</sup>)-linked bis(pyrimidinenorcorrole) **1** which in solution exists in

equilibrium with a monomeric radical (see picture). After dehydrogenation **1** shows a conformation-dependent singlet–triplet equilibrium.